American Journal of Bioscience and Bioinformatics (AJBB)

ISSN: 2995-0481 (ONLINE)

VOLUME 4 ISSUE 1 (2025)

PUBLISHED BY
E-PALLI PUBLISHERS, DELAWARE, USA

American Journal of Bioscience and Bioinformatics (AJBB)

Volume 4 Issue 1, Year 2025
ISSN: 2995-0481 (Online)
DOI: https://doi.org/10.54536/ajbb.v4i1.4516
https://journals.e-palli.com/home/index.php/ajbb

In Vivo Antiplasmodial Studies of *Achyranthes Aspera* Fractions and Molecular Docking Studies of Its Phytochemicals against *Plasmodium* Aspartic Proteases Targeted in Antimalarial Drug Design

Mary Matawal Mankilik[1*], Joel Paul[1], Daniel Hassan Mhya[2], Carrol Domkat Luka[1], Ishaya Yohanna Longdeta[1]

Article Information

Received: February 06, 2025
Accepted: March 10, 2025
Published: May 12, 2025

Keywords

4-(3-Hydroxy-1-Propenyl-2-) Methoxy, Achyranthes Aspera, Antiplasmodial Activity Molecular Docking, Rotundioside B

ABSTRACT

Evaluation of fractionated extracts of *Achyranthes aspera* L. as an alternative antimalarial therapy is essential due to the increasing resistance of *Plasmodium falciparum* to artemisinin. The side effects, limited accessibility, and high cost of current drugs have intensified interest in phytochemical screening of medicinal plants as sources of bioactive compounds with antimalarial properties. The mode of action of these phytochemicals remains largely unknown, necessitating an investigation into their in vivo antimalarial activity and in silico molecular interactions with Aspartic Proteases (Plasmepsin I, II, and IV), key drug targets in malaria treatment. The in vivo antiplasmodial activity of *Achyranthes aspera* fractions was assessed using Rane's curative assay in a mouse model infected intraperitoneally with $1x10^7$ *Plasmodium berghei* (NK-65) parasitized RBCs per milliliter, while LC-MS techniques analyzed the phytochemical composition. In silico drug-likeness studies, including PASS, molecular docking, ADME/Tox, and Lipinski's rule of five, were conducted, with chemical compounds docked against Plasmepsins I, II, and IV. Rane's curative test showed significant ($P<0.05$) parasite reduction, with the chloroform fraction achieving more than 50% reduction at 200 mg/kg b.wt. LC-MS identified 37 compounds, 11 of which demonstrated plasmepsin inhibitory activity. Docking studies predicted Rotundioside B and 4-(3-hydroxy-1-propenyl-2-) methoxy as the most effective, exhibiting favourable binding energies. In silico ADMET analysis confirmed good oral bioavailability and drug-likeness properties. Findings indicate that *A. aspera* shoot fractions possess antiplasmodial activity, with the chloroform fraction significantly reducing *P. berghei* burden in a manner comparable to artemisinin-based combination therapy (ACT), supporting its potential for pharmaceutical drug development.

INTRODUCTION

Malaria, a life-threatening disease caused by *Plasmodium* parasites and transmitted by Anopheles mosquitoes, affected about 241 million people and claimed almost 627000 lives in 2020, with resistance to artemisinin combination therapy (ACT), the standard treatment for *Plasmodium falciparum*, posing a growing global threat due to Pfkelch13 gene mutations (WHO, 2021; Ashley *et al.,* 2014). This resistance, alongside vector insecticide challenges and diagnostic setbacks from pfhrp2/3 mutations, highlights the urgent need for new antimalarial agents targeting novel pathways (Menard *et al.,* 2016; WHO, 2021). *Achyranthes aspera*, a medicinal plant from the Amaranthaceae family, has the potential to be an alternative for malaria treatment. Therefore, this research seeks to evaluate the in vivo antimalarial effects of *Achyranthes aspera* and identify the lead compounds that targets *Plasmodium* proteases (plasmepsins) to combat artemisinin resistance.

LITERATURE REVIEW

The battle against malaria has been shaped by extensive research into the efficacy of antimalarial drugs and the challenges posed by resistance. Artemisinin combination therapy (ACT) has been the cornerstone of *P. falciparum* treatment due to its rapid parasite clearance and transmission reduction capabilities. However, its effectiveness is increasingly undermined by treatment failures, first noted in Southeast Asia (Ashley *et al.,* 2014). Studies attribute this resistance to point mutations in the Pfkelch13 gene of *P. falciparum*, with evidence of its global spread raising alarms about future therapeutic options (Menard *et al.,* 2016; Noedl *et al.,* 2008; Dondorp *et al.,* 2009). Kamau *et al.* (2014) suggest that while Pfkelch13 mutations are a primary driver, some resistance mechanisms remain unresolved, complicating drug development efforts. Additionally, vector insecticide resistance and genetic changes in *Plasmodium falciparum* histidine-rich protein 2 (pfhrp2) and *Plasmodium falciparum* histidine-rich protein 3 (pfhrp3) genes have led to false negative test results, further hindering malaria control (WHO, 2021). These challenges have spurred investigations into alternative targets and agents to overcome the limitations of current therapies (Fidock *et al.,* 2008).

The *plasmodium* proteases such as aspartic proteases (plasmepsins) have emerged as viable druggable targets due to their essential role in haemoglobin degradation during the parasites blood stage (Francis *et al.,* 1997). Of the ten identified plasmepsins, types I, II, and IV are critical in the early stages of this process (Coombs *et al.,* 2001). Proteases also facilitate erythrocyte rupture and reinvasion, making them attractive for therapeutic intervention (Rosenthal,

[1] Department of Biochemistry, Faculty of Basic Medical Sciences, College of Health Sciences, University of Jos, Jos, Plateau State, Postcode - 930003, Nigeria
[2] Department of Medical Biochemistry, Abubakar Tafawa Balewa University, Bauchi, Nigeria
[*] Corresponding author's e-mail: mankilikma@unijos.edu.ng

1998; Pandey & Dixit, 2012). However, the high similarity among food vacuole plasmepsins has obscured their specific in vivo roles, posing challenges to targeted drug design (Liu *et al.,* 2014; Moura *et al.,* 2009; Berry, 1997). Current antimalarial drugs predominantly target the blood stage, but their reliance on traditional targets limits efficacy against resistant strains, necessitating exploration of new molecular pathways (Wilson *et al.,* 2013; Rasmussen *et al.,* 2021; Shibeshi *et al.,* 2020).

Medicinal plants have long been a rich source of bioactive compounds, with pharmaceutical research leveraging molecular modeling and synthetic chemistry alongside natural products (Balunas & Kinghorn, 2005). *Achyranthes aspera*, a tropical weed from the Amaranthaceae family, is renowned for its diverse phytochemicals and biological activities, including immunomodulatory (Rao *et al.,* 2002), wound healing (Alam *et al.,* 2004), antioxidant (Priya *et al.,* 2010), anti-inflammatory (Kumar *et al.,* 2009), antibacterial (Alam *et al.,* 2009), and antifungal effects (Elumalai *et al.,* 2009). Recent studies have confirmed the antimalarial efficacy of its aqueous and methanolic shoot extracts (Mankilik *et al.,* 2021), supporting its traditional use as an antimalarial agent (Burkill, 1985; Jain *et al.,* 2006). Phytochemical analyses reveal compounds responsible for these activities (Saurabh *et al.,* 2011), positioning *A. aspera* as a candidate for identifying novel antimalarial leads. This study builds on these findings by hypothesizing that *A. aspera* fractions could inhibit plasmepsins and exhibit significant in vivo malarial activity, offering a potential solution to artemisinin resistant malaria.

MATERIALS AND METHODS

Plant Collection and Identification

Fresh shoot of *Achyranthes aspera* Linn were harvested from 'Nchiya' village in Mangu LGA, Plateau State in August 2017. Shoots were wrapped in a plastic sheet during transport. Plant identification and voucher specimen reference (32180) were done in the Department of Botany herbarium in the Forestry Research Institute in Nigeria (FRIN) by a taxonomist.

Chemicals

All chemicals and reagents used were of analytical grade purchased from Sigma Aldrich USA.

Experimental Animals

Swiss albino mice of both sexes with age range of about 6-8 weeks, weighing 16-22g were used for the study. The mice were obtained from animal house unit of Pharmacology Department, Faculty of Pharmaceutical Sciences, University of Jos, Nigeria. All experimental mice were housed under standard environmental conditions. They were fed with vital feeds (ECWA Feeds, Jos) and clean water *ad libitum*.

Ethical Statement

Ethical approval of this study was given by the ethical committee animal house unit of the Department of Pharmacology, Faculty of Pharmaceutical Sciences with an approval number UJ/FPS/F17-00379. All experimental protocols were carried out in line with National and International laws and guidelines for care and use of laboratory animals in principle of laboratory animal care (NIH, 1985) (National Research Council, 2011).

Parasite and Inoculation of *P. berghei* in Mice

Chloroquine-sensitive *Plasmodium berghei* (NK-65) was sourced from the National Institute of Medical Research (NIMR) at the University of Ibadan, located in Uyo State, Nigeria. The parasite was sustained by weekly serial transfers of infected blood between mice. For the in vivo malaria curative study of the plant fraction, a donor mouse exhibiting a parasitemia of 20–30% was selected to infect the experimental mice. To prepare the inoculum, the donor mouse's parasitemia was first assessed. The mouse was then mildly anesthetized using chloroform-soaked cotton wool and euthanized. Its blood was collected in a Petri dish with 2% trisodium citrate to prevent clotting. The blood was diluted with 0.9% normal saline to achieve a concentration where each 0.2 ml sample contained approximately 1 x 107 *berghei*-infected red blood cells (RBCs), while a 1 ml inoculum contained 5 x 10^7 infected erythrocytes. Each test mouse received an intraperitoneal injection of 0.2 ml of this diluted blood (Fidock *et al.,* 2008).

Preparation of Methanolic Extracts

About 500 g of coarsely powdered shoot of *Achyranthes aspera* was weighed on sensitive digital weighing balance (Ohaus, USA) and extracted by cold maceration technique with methanol (500 g in 4800 ml) in the ratio of 1:9 in Erylenmeyer flask. The plant materials were extracted using an orbital shaker (Gallenkamp) at 120 rpm for 72 hours. The resulting extract was initially filtered through gauze to remove the marc, followed by filtration through Whatman No. 1 filter paper (150 mm, Wagtech International Ltd.). The marc was re-extracted twice with methanol to ensure complete extraction. The combined methanol extracts were then concentrated to dryness using a rotary evaporator (RES2-1, Switzerland) at 40°C and 80 rpm, yielding 101.33 g of crude extract. The extract was stored at -20°C in screw-cap vials until further use. (Tiwari, Kumar & Kaur, 2011).

Fractionation of Methanolic Extract

The crude methanolic extract Solvent-solvent fractionation was performed based on the method described by Yared *et al.* (2012). Eight grams of powdered methanolic extract was suspended in 20 mL of distilled water within a separating funnel. This suspension was then subjected to sequential partitioning with n-hexane, chloroform, and n-butanol, in order of increasing polarity. Three extractions, each using 200 mL of solvent, were performed for each partitioning step. The combined n-hexane extracts were concentrated at 40°C, yielding 1.94g of the hexane fraction (HF). The remaining

aqueous layer was then partitioned with chloroform, and the combined chloroform extracts were concentrated, resulting in 0.74g of the chloroform fraction (CF). Following this, the aqueous layer was partitioned with n-butanol, and the combined butanol extracts were concentrated, yielding 0.82g of the butanol fraction (BF). Finally, the remaining aqueous fraction was dried, resulting in 1.87g. All fractions were stored in tightly sealed stainless-steel containers at -20°C until use in in vivo testing. For these tests, the CF was dissolved in 2% Tween 80, while the HF, BF, and aqueous fraction were dissolved in water.

Animal Groupings and Treatment

A total of 85 mice were randomly assigned to nine groups, with five mice per group. This included four treatment groups and five control groups. The vehicle control group was administered 2% Tween 80, which served as the reconstitution solvent for the chloroform fraction. Positive control groups received either chloroquine at 10 mg/kg/day or ACT at 25 mg/kg/day. The treatment groups received varying doses of the plant fractions: 100, 200, or 400 mg/kg/day of the hexane, chloroform, n-butanol, and aqueous fractions. The selection of these doses was informed by prior safety and toxicity studies, as detailed in Mankilik *et al.* (2021).

Activity Testing (in Vivo Anti-malarial Test)

The in vivo antiplasmodial activity of the plant fraction against established *P. berghei* infection was carried using a method of Ryley and Peters (1970). Mice were inoculated with parasitized erythrocytes on the first day (Day 0) seventy-two hours later (on day 3) the mice were randomly grouped and treated, and the treatment continued for four consecutive days from day three up to day six once daily. Parameters including parasitemia rectal temperature (using digital rectal thermometer) and body weight were measured (before treatment and after treatment). PCV were recorded on day three and day seven. Finally, survival time of the experimental mice in each treatment groups were followed and determined

Packed Cell Volume Determination

To evaluate the extracts and fractions' ability to prevent hemoglobin reduction associated with increasing parasitemia in malaria, PCV was measured. The PCV, which represents the proportion of red blood cells in total blood volume and is used to estimate mean erythrocyte hemoglobin concentration, was determined using a modified Wintrobe's method. Blood samples were obtained from the tails of mice using heparinized micro-hematocrit tubes. These tubes were filled to three-quarters of their capacity and sealed with crystoseal. The sealed tubes were then centrifuged at 12,000 rpm for five minutes in a micro-hematocrit centrifuge, with the sealed end facing outwards. Following centrifugation, PCV values were determined using a hematocrit reader. Baseline PCV measurements were taken prior to parasite inoculation using Equation 1.

Packed Cell Volume (PCV) =(Volume of erythrocytes in a given volume of blood)/(Total blood volume) (1)

Determination of Parasitemia

Thin blood smears were prepared from the tail blood of the mice in the test and control groups using microscopic slides. After air-drying, the smears were fixed with methanol (absolute) and stained with 10% Giemsa stain at pH 7.2 for 15 minutes. The stained slides were gently washed with tap water and air-dried at room temperature. With a drop of immersion oil, the number of parasitized red blood cells (PRBCs) was counted using a light microscope (Olympus CH) at 100x magnification. Five fields were counted, recording the number of infected and uninfected red blood cells, and the average count was determined. The mean parasitemia was calculated according to CDC - DPDx - Diagnostic Procedures - Blood Specimens, 2019. (Assuming *Plasmodium* infection, the number of *Plasmodium* infected red blood cells were counted).

Parasitemia = [(Total number of parasitized red blood cells (pRBC))/(Total number of Red blood cells (No.of parasitized+ No.of Uninfected RBCs))] x 100% (2)

Finally, the amount of reduction in parasite in the curative test using the fractions was compared with respect to the controls.

Determination of Mean Survival Time

The duration of survival was tracked to assess how the extracts and fractions influenced the extension of survival days. The Mean Survival Time (MST) was calculated for both the treatment and control groups by averaging the survival time (in days) of mice following inoculation, observed over a 30-day period (D0-D29). According to established criteria, a compound is considered active if it extends survival beyond 12 days. The MST for the mice, measured in days, was determined using Equation 3.

MST = (Sum of survival time for all mice in a group (in days))/(Total number of mice in the group) (3)

Determination of Body Weight

The body weight of the mice (in grams) was measured with a sensitive weighing balance 3 hours before infection and throughout the treatment period in the curative test, to evaluate if the plant extracts and fractions could mitigate weight loss. The body weight, expressed in grams, was determined using Equation 4.

Mean Body Weight = (Total weight of Mice in a group)/(Total number of mice in that group) (4)

Measurement of Rectal Body Temperature

The rectal temperature of each mouse was recorded using a digital thermometer one hour prior to infection to assess the potential impact of the extracts and fractions on temperature regulation during a 5-day curative test. It is widely recognized that, unlike in humans, the rectal temperature of mice drops sharply as parasitemia

increases. The effectiveness of the extracts and fractions was evaluated based on their ability to prevent this rapid temperature decline.

Isolation and Characterization of Chloroform Fraction

The chloroform's fractions were purified using flash chromatography with silica gel (60-120 mesh). A homogeneous silica gel slurry was prepared by mixing silica gel with n-hexane and stirring to remove air bubbles. This slurry was then poured into a glass column. A sample of 3.65g of the chloroform fraction was dissolved in 50mL of n-hexane for loading. Prior to flash chromatography, a preparative thin-layer chromatography (TLC) separation was performed using a chloroform:methanol (99:1) mobile phase. The fraction was mixed and dried with 10g of silica gel at room temperature. This dried silica/chloroform fraction mixture was then layered onto the column bed. The column was eluted with a gradient of increasing polarity, starting with n-hexane and increasing chloroform concentration by 5% increments. Once 100% chloroform was reached, the methanol concentration was increased by 5% increments. Fractions were collected in glass beakers and pooled based on their TLC profiles, resulting in nine subfractions. These subfractions were concentrated to dryness at room temperature, stored in sterile bottles, and subsequently analyzed by LC-MS for compound identification and characterization.

LC-MS Analysis of Chloroform Fraction Subfraction

The chloroform subfractions were analyzed using high-performance liquid chromatography-mass spectrometry (HPLC-MS). For analysis, 0.5-1.0 mg/mL of each subfraction was dissolved in methanol and filtered through a 0.45 µm membrane filter prior to injection into the HPLC-MS system. The HPLC system was an Agilent 1260 Infinity, equipped with a UV detector (wavelength 220-270 nm), an autosampler (1 µL injection volume), and a thermostated column (Phenomenex Kinetex XB-C18, 50 x 4.6 mm, 2.6 µm) maintained at 40°C. The mobile phase consisted of 99.9% acetonitrile with 0.1% acetic acid for both mobile phases A and B, delivered at a flow rate of 2 mL/min. Mass spectrometry was performed using an Agilent 6130 single quadrupole mass spectrometer (scanning in ES+/APCI mode over 70-1100 m/z) and an Agilent 1290 Infinity evaporative light scattering detector (ELSD). The data acquisition and processing were analysed with agilent Mass Hunter software was used. Compounds in the chloroform subfractions were tentatively identified by comparing their monoisotopic and exact masses, mass spectral fragmentation patterns, and reference literature.

Prediction of Biological Activities of *A. aspera* Shoot Phytochemicals

To assess the general biological activity of the identified plant shoot phytochemicals, Prediction of Activity Spectra for Substances (PASS) analysis was employed. Chemical similarity searches were conducted on PubChem for all 37 compounds identified through LC-MS. This search provided canonical SMILES and PubChem CID information. The detailed compound information was then downloaded in SDF format.

Preparation of Ligand (Phytochemicals)

Based on PASS analysis, 11 molecules identified from *A. aspera* shoots were retrieved from PubChem (http://www.ncbi.nlm.nih.gov./pccompound) in 3D SDF format. These molecules were then converted to PDBQT format for AutoDock.

Preparation of Protein for Docking Studies

Molecular docking using AutoDock Vina 4.2 was performed to examine the nature of interactions, binding modes, and selectivity of compounds derived from the *A. aspera* shoot chloroform fraction with malaria-associated enzymes, specifically plasmepsins I, II, and IV. Ligand PDBQT files were generated from the compounds' retrieved PDB files using AutoDock Tools. The 3D structures of the target enzymes, plasmepsin I (PDB ID: 3QRV), plasmepsin II (PDB ID: 2BJU), and plasmepsin IV (PDB ID: 5JOD), were obtained from the Protein Data Bank (PDB). Prior to docking, water molecules were removed from the protein structures, and polar hydrogens and charges were added using AutoDock Tools, as described by Khodade *et al.* (2007). These modified protein structures were then saved in PDBQT format.

Molecular Docking of Phytochemicals with Plasmepsin

To determine the inhibitory potential of *A. aspera* phytochemicals against plasmepsins I, II, and IV, molecular docking studies were performed. Phytochemical ligands were docked with the selected parasite enzymes using AutoDock Tools. The resulting docking energies (kcal/mol) were generated, and those indicating favorable binding were identified.

In Silico Pre-Clinical Testing of Plant Shoot Phytochemicals

To evaluate the adsorption, distribution, metabolism, excretion, and toxicity (ADMET) properties of the plant shoot phytochemicals, ADMET-TOX_Drug4, a freely available ADME-Tox tool, was utilized (Lagorce *et al.,* 2017). The drug-likeness of the phenolic compounds was determined using the Lipinski filter online server, which assesses properties such as the octanol/water partition coefficient (cLogP), hydrogen bond donors/acceptors, and molar refractivity (Taylor & Francis, 2021).

Option 3 (Focus on the Two Parts)

Statistical Analysis

Statistical analysis of the data was performed using SPSS software, version 22.0, using ANOVA to compare results between groups. Data are presented as the mean ± standard error of the mean (SEM). For the in vivo antimalarial studies, statistical significance was determined at a P-value of less than 0.05. Additionally, bioinformatics analyses were conducted.

RESULTS AND DISCUSSION

Phytochemical Screening

Phytochemical screening of *A. aspera* shoot fractions shown in Table 1 demonstrated the presence of multiple phytoconstituents across all fractions. Notably, alkaloids were detected in all fractions. These results are consistent with the phytochemical profiles reported by Tiwari *et al.* (2018). The ubiquitous presence of alkaloids suggests a potential role in the observed ant plasmodial activity. Furthermore, high levels of saponins were observed, which may also contribute to the antimalarial activity, either independently or in synergy with other compounds, as documented by Mankilik *et al.* (2021).

Antiplasmodial Activity of The Solvent Fraction

The solvent fractions of *A. aspera* significantly reduced parasitemia ($P < 0.05$) across various doses when compared to the negative control, although a consistent dose-dependent relationship was not apparent. The butanol fraction, administered at 100 mg/kg, exhibited significant antiplasmodial activity (Figure 1). The chloroform fraction at 200 mg/kg demonstrated activity comparable to the standard drug artesunate (Figure 2), and the aqueous fraction at 400 mg/kg showed significant antiplasmodial activity as seen in Figure 3 below. All three tested doses displayed statistically significant differences from the untreated control and were compared to the artesunate treated group. The *P. berghei* rodent malaria model is widely used for initial in vivo screening of antimalarial compounds (Fidock *et al.,* 2008). These results are consistent with previous reports indicating promising antimalarial properties of *A. aspera* extracts (Mankilik *et al.,* 2021; Longdet *et al.,* 2019). The observed difference in activity, with the chloroform fraction showing greater parasite reduction at 200 mg/kg than the hexane fraction at 100 mg/kg, underscores the variability in antimalarial efficacy among different solvent fractions.

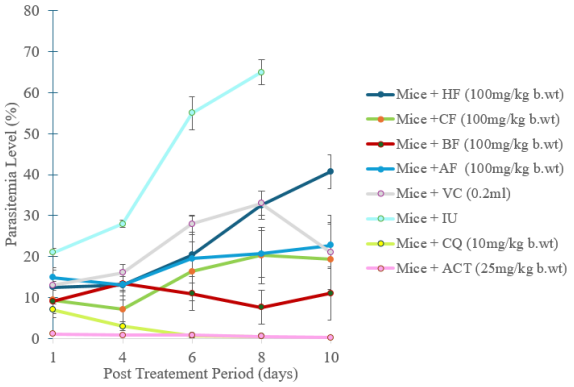

Figure 1: Parasitemia Level of Mice Infected with *Plasmodium berghei* (NK-65) and Treated with Fractions of *A. aspera* at Low Dose.

Mice + AF represents infected mice treated with the aqueous fraction of *Achyranthes aspera*, Mice + HF represents infected mice treated with the hexane fraction of *Achyranthes aspera*, Mice + CF represents infected mice treated with the chloroform fraction of *Achyranthes aspera*, Mice + BF represents infected mice treated with the butanol fraction of *Achyranthes aspera*, Mice + VC represents the vehicle control (0.2 mL), mice + IU represents infected, untreated mice, Mice + CQ represents infected mice treated with chloroquine (10 mg/kg), and Mice + artesunate represents infected mice treated with artesunate (25 mg/kg).

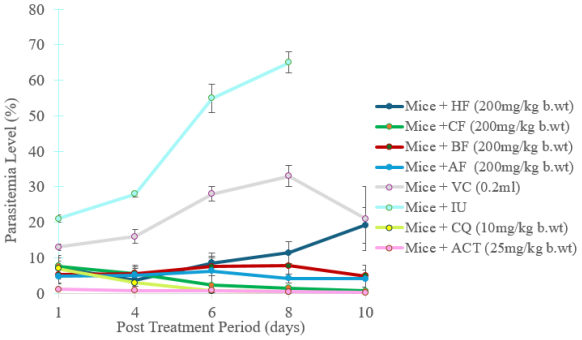

Figure 2: Parasitemia Level of Mice Infected with *Plasmodium berghei* (NK-65) and Treated with *Achyranthes aspera* Fractions at Median Dose.

Mice + AF represents infected mice treated with the aqueous fraction of *Achyranthes aspera*, Mice + HF represents infected mice treated with the hexane fraction of *Achyranthes aspera*, Mice + CF represents infected mice treated with the chloroform fraction of *Achyranthes aspera*, Mice + BF represents infected mice treated with the butanol fraction of *Achyranthes aspera*, Mice + VC represents the vehicle control (0.2 mL), Mice + IU represents infected, untreated mice, Mice + CQ represents infected mice treated with chloroquine (10 mg/kg), and Mice + artesunate represents infected mice treated with artesunate (25 mg/kg).

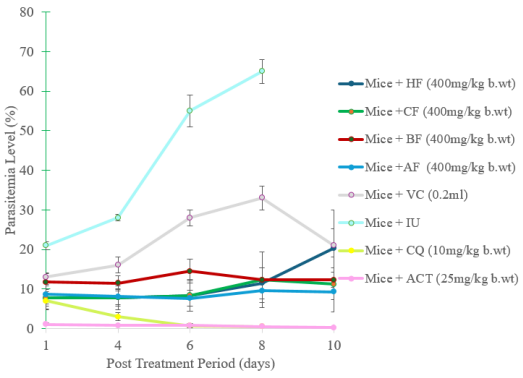

Figure 3: Parasitemia Level of Mice Infected with *Plasmodium berghei* (NK-65) and Treated with *Achyranthes aspera* Fractions at High Dose

Mice + AF represents infected mice treated with the aqueous fraction of *Achyranthes*, Mice + HF represents infected mice treated with the hexane fraction of *Achyranthes*, Mice + CF represents infected mice treated

with the chloroform fraction of *Achyranthes*, Mice + BF represents infected mice treated with the butanol fraction of *Achyranthes*, Mice + VC represents the vehicle control (0.2 mL), Mice + IU represents infected, untreated mice, Mice + CQ represents infected mice treated with chloroquine (10 mg/kg), and Mice + ACT represents infected mice treated with artesunate (25 mg/kg).

Packed Cell Volume

All *Achyranthes* fractions at low (Figure 4), medium (Figure 5), and high doses (Figure 6) were shown to have protected effect against PCV reduction. The chloroform fraction at 200 mg/kg significantly ameliorated PCV reduction compared to the negative control. This protective effect may be due to the plant's ability to reduce malaria-induced haemolysis.

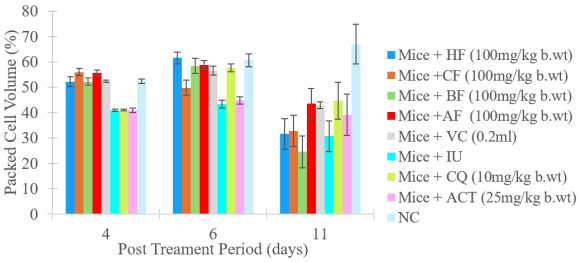

Figure 4: Packed Cell Volume of Mice Infected with *Plasmodium berghei* (NK-65) and Treated with Fractions (Low Dose) of *Achyranthes aspera*

Mice + HF represents infected mice treated with the hexane fraction of *Achyranthes*, Mice + CF represents infected mice treated with the chloroform fraction of *Achyranthes*, Mice + BF represents infected mice treated with the butanol fraction of *Achyranthes*, Mice + AF represents infected mice treated with the aqueous fraction of *Achyranthes*, Mice + VC represents the vehicle control (0.1 mL), Mice + IU represents infected, untreated mice, Mice + CQ represents infected mice treated with chloroquine (10 mg/kg), Mice + ACT represents infected mice treated with artesunate (25 mg/kg), and NC represents the normal control group.

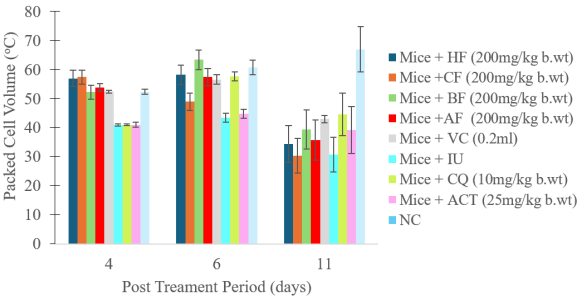

Figure 5: Packed Cell Volume of Mice infected with *Plasmodium berghei* (NK-65) and Treated with Fractions (Median Dose) of *Achyranthes aspera*

Mice + HF represents infected mice treated with the hexane fraction of *Achyranthes*, Mice + CF represents infected mice treated with the chloroform fraction of *Achyranthes*, Mice + BF represents infected mice treated with the butanol fraction of *Achyranthes*, Mice + AF represents infected mice treated with the aqueous fraction of *Achyranthes*, Mice + VC represents the vehicle control (0.1 mL), Mice + IU represents infected, untreated mice, Mice + CQ represents infected mice treated with chloroquine (10 mg/kg), Mice + ACT represents infected mice treated with artesunate (25 mg/kg), and NC represents the normal control group.

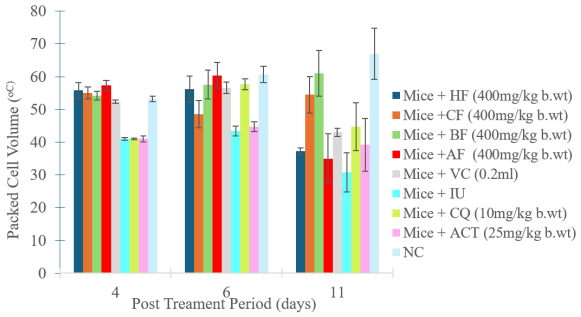

Figure 6: Packed Cell Volume of Mice infected with *Plasmodium berghei* (NK-65) and Treated with Fractions (High Dose) of *Achyranthes aspera*

Mice + HF represents infected mice treated with the hexane fraction of *Achyranthes*, Mice + CF represents infected mice treated with the chloroform fraction of *Achyranthes*, Mice + BF represents infected mice treated with the butanol fraction of *Achyranthes*, Mice + AF represents infected mice treated with the aqueous fraction of *Achyranthes*, Mice + VC represents the vehicle control (0.1 mL), Mice + IU represents infected, untreated mice, Mice + CQ represents infected mice treated with chloroquine (10 mg/kg), Mice + ACT represents infected mice treated with artesunate (25 mg/kg), and NC represents the normal control group.

Mean Survival Time

Administration of *Achyranthes* solvent fractions to infected mice resulted in a prolongation of survival time, with mean survival times ranging from 10 to 15.5 days, in contrast to the control group. A statistically significant increase in survival time ($P < 0.05$) was observed at higher doses, as depicted in Figure 7. Notably, the chloroquine-treated group exhibited the longest mean survival time, reaching 28 days. The observed extension of survival time indicates a reduction in the pathological effects caused by the parasites, which aligns with findings from previous studies (Mankilik *et al.,* 2021; Longdet *et al.,* 2019).

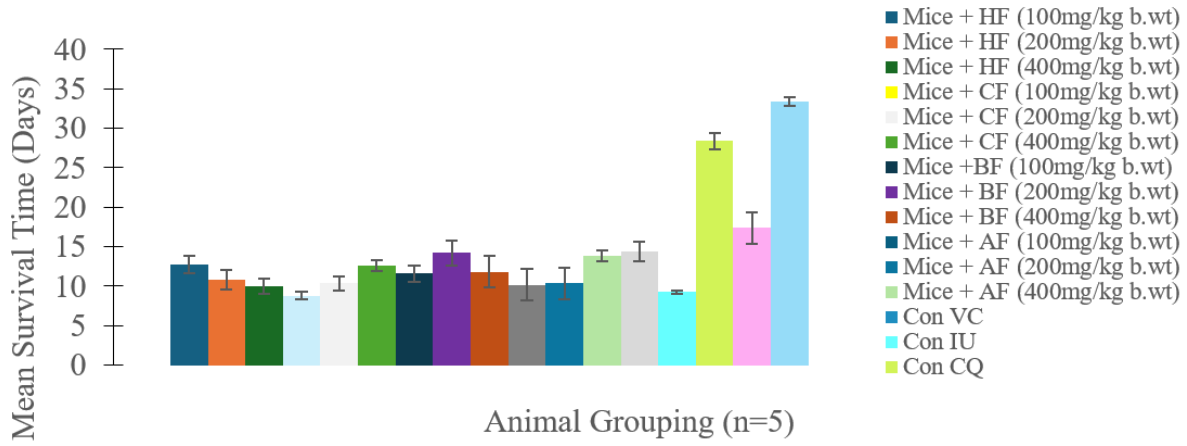

Figure 7: Mean Survival Time of Infected Mice at Varied Doses of *Achyranthes aspera* Fractions

Mice + AF represents infected mice treated with the aqueous fraction of *Achyranthes*, Mice + HF represents infected mice treated with the hexane fraction of *Achyranthes*, Mice + CF represents infected mice treated with the chloroform fraction of *Achyranthes*, Mice + BF represents infected mice treated with the butanol fraction of *Achyranthes*, Mice + VC represents the vehicle control (0.2 mL), Mice + IU represents infected, untreated mice, Mice + CQ represents infected mice treated with chloroquine (10 mg/kg), Mice + ACT represents infected mice treated with artesunate (25 mg/kg), NC represents the normal control group, NT represents not treated, and ND represents no dose.

Body Temperature of Mice

As shown in Figure 8, all fractions of *Achyranthes aspera* effectively prevented a reduction in rectal temperature in *P. berghei*-infected mice. Specifically, at doses of 100, 200, and 400 mg/kg body weight, all fractions, with the exception of the hexane and chloroform fractions at 400 mg/kg, prevented a decline in temperature when compared to mice treated with artesunate and chloroquine. Fluctuations in body temperature are indicative of changes in metabolic rate, and effective antimalarial substances are expected to counteract temperature reductions (Chilombe *et al.,* 2022; Clarke, 2004; Protsiv *et al.,* 2020).

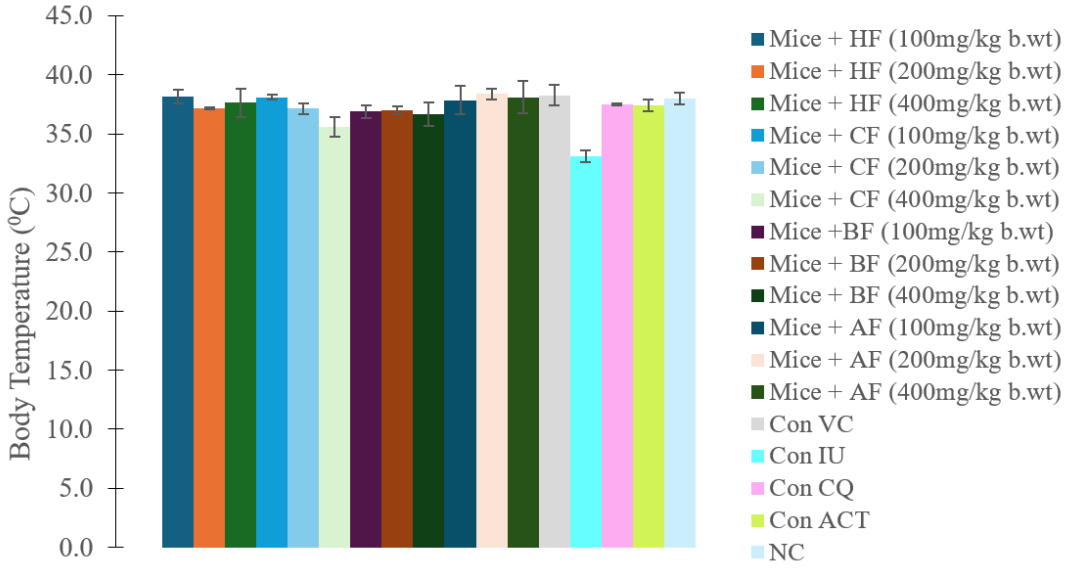

Figure 8: Rectal Body Temperature of Infected Mice Treated with Varied Doses of Fractions of *Achyranthes aspera*

Mice + HF represents infected mice treated with the hexane fraction of *Achyranthes*, Mice + CF represents infected mice treated with the chloroform fraction of *Achyranthes*, Mice + BF represents infected mice treated with the butanol fraction of *Achyranthes*, Mice + AF represents infected mice treated with the aqueous fraction of *Achyranthes*, Mice + VC represents the vehicle control (0.2 mL), Mice + IU represents infected, untreated mice, Mice + CQ represents infected mice treated with chloroquine (10 mg/kg), Mice + ACT represents infected mice treated with artesunate (25 mg/kg), NC represents the normal control group, NT represents not treated, and ND represents no dose.

Body Weight

Figure 9 demonstrates that all *Achyranthes aspera* fractions prevented body weight loss compared to the negative control, but the effect varied with dose. The aqueous fraction at 100 mg/kg showed the greatest prevention, while the chloroform fraction at 400 mg/kg showed the least. This suggests a potential dose-dependent effect, possibly due to appetite suppression from phytochemicals like phenolics, saponins, flavonoids, or tannins (Davkova *et al.,* 2024; López-Yerena *et al.,* 2020; Saglam & Sekerler, 2024; Sahib *et al.,* 2012).

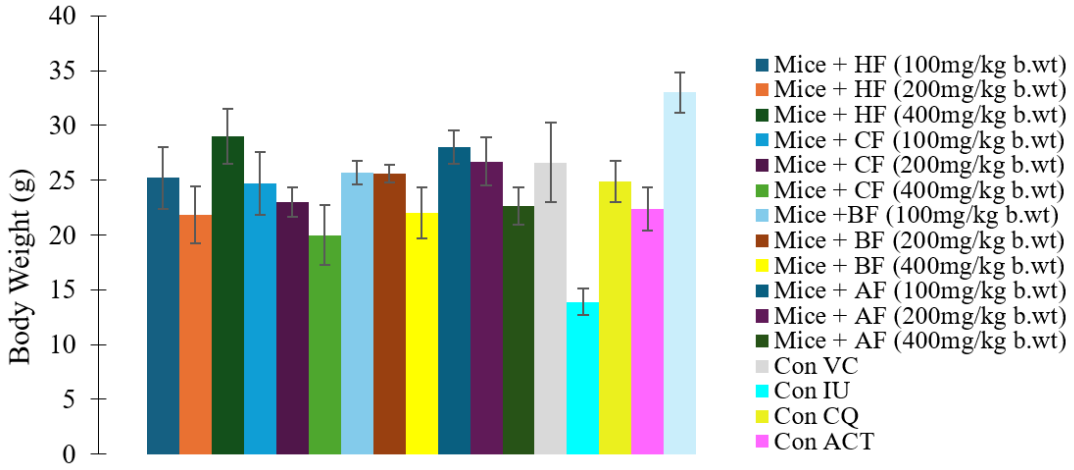

Figure 9: Body Weight of Infected Mice treated with Varied Doses of Fractions of *Achyranthes aspera*

Mice + HF represents infected mice treated with the hexane fraction of *Achyranthes*, Mice + CF represents infected mice treated with the chloroform fraction of *Achyranthes*, Mice + BF represents infected mice treated with the butanol fraction of *Achyranthes*, Mice + AF represents infected mice treated with the aqueous fraction of *Achyranthes*, Con VC represents the vehicle control (0.2 mL), Con IU represents infected, untreated mice, Con CQ represents infected mice treated with chloroquine (10 mg/kg), Con ACT represents infected mice treated with artesunate (25 mg/kg), and NC represents the normal control group (see Appendix B9)

LC-MS Analysis

LC-MS analysis of the *A. aspera* shoot chloroform fraction consistently identified 37 compounds, primarily saponins, flavonoids, alcohols, phenols, and steroids (Table 1). Key constituents included gypsogenic acid (99.0%), oleanolic acid (100%), betaine (100%), chikusetsusaponin IVa (87%), spathulenol (4%), rotundioside B saponin (37.02%), 5,7-dimethoxyflavon-O-α-6-8-rhamnopyranosyl glycoside (22.4%), betulinic acid (30.0%), and α-spinasterol-3-glycoside (29.5%). These results align with previous studies reporting similar phytochemical profiles in *A. aspera* (Chileh-Chelh *et*

Table 1: LC_MS Analysis of Bioactive Components in Chloroform Fraction of *A. asperaShoot*

S/N	RT/min	Name of Compound	Molecular Formular	Molecular Weight	Peak Area (%)
1.	0.265	Gypsogenic acid (Pentacyclictriterpenoid saponins	$C_{30}H_{46}O_5$	486	99.0
2.	1.927	Spathulenol (Alkaloid)	$C_{15}H_{29}O$	220	40.0
3.	2.006	Dibuthylphathalate (ester of pthalic acid)	$C_{16}H_{22}O_4$	278	3.7
4.	8.460	Dexapanthenol (alcohol)	$C_9H_{19}NO_4$	205	16.2
5.	6.589	Chikutsesusaponin iva (tripertene saponin)	$C_{42}H_{66}NO_4$	794	87.0
6.	6.602	Betain (flavonoid)		550	37.8
7.	4.727	4-(3-hydroxy-1-propenyl-2-methoxy (phenol)	$C_{20}H_{40}O$	180	6.7
8.	6.909	1-pentacontanol phosphate ester	$C_{50}H_{105}O_5P$	815	100
9.	5.481	Phytol (diterpene alcohol)	$C_{20}H_{40}O$	296	0.3
10.	6.049	5,7, dimethoxyflavone -4-0-alpha-6-rhamnopyranosyl glycosyl (flavonoids)	$C_{17}H_{14}O_4$	609	33.4
11.	6.575	Hydroxyphytolaccagenin (saponin)	$C_{36}H_{56}O_{11}$	547	18.2
12.	8.477	Quercetin monoisotopic (flavonoids)	$C_{15}H_{12}O_8$	755	16.0
13.	5.488	α-spinasterol-3-glycoside (steroids)	$C_{35}H_{58}O_6$	574	29.5
14.	5.186	Keampferol 3-0-galactoside (flavonoids)	$C_{21}H_{20}O_{11}$	448	10.4

15.	5.054	Cauasapogenin (saponin)	$C_{30}H_{48}O_4$	472	1.3
16.	6.607	Lutein	$C_{40}H_{56}O_2$	568	14.0
17.	8.472	Eugenol acetate (phenol)	$C_{12}H_{12}O_3$	206	16.2
18.	8.466	Tetraflourenthylene	C_2F_4	100	11.0
19.	0.224	Oleonolic acid (triterpenaglycone saponin)	$C_{30}H_{48}O_3$	456	100
20.	0.224	Lupeol (triterpene)	$C_{30}H_{50}O$	426	
21.	4.949	Hexatriacontane II methyl	$C_{37}H_7O$	521.0	12.1
22.	5.054	Gypsigenin-3-0-D glucoronide (saponin)	$C_{36}H_{54}O_{10}$	646	13.6
23.	0.261	Betaine (flavonoid)	$C_5H_{11}NO_2$	117	100
24.	5.062	Acetoxy-6-benzoxyloxy apangamide	$C_4H_6O_4$	586	16.7
25.	0.565	Tetradecane (alkane)	$C_{14}H_{30}$	198	7.0
26.	6.704	Squalene (vitamin E)	$C_{30}H_{50}$	410	2.1
27.	2.081	9,12-octadecanoic acid (z, z) (linoliec acid)	$C_{18}H_{32}O_2$	280	6.3
28.	2.006	Rotundioside B (triterpenoid Saponin/ tetrassaccharide of oleonolic acid)	$C_{54}H_{87}O_{26}S$	1184.3	37.02
29.	5.064	27-cyclohexy-hepacosy-7-ol	$C_{27}H_{44}O_2$	400	3.1
30.	1.356	17-Pentatriacontane (Alkane)	$C_{35}H_{75}$	408	3.0
31.	1.725	Hepta-cosan-2-one (ketone)	$C_{29}H_{54}O$	396	2.3
32.	2.008	Triacontanol (Aliphatic alcohol)	$C_{30}H_{62}O$	438	0.8
33.	2.231	Pentatriacontane (Alkane)	$C_{35}H_{72}$	492	2.9
34.	8.279	Gypsogenin - 3 – 0-D glucoronides (saponins)	$C_{34}H_{56}O$	660	0.3
35.	1.043	α-ionone (compound of volatile oil)	$C_{13}H_{20}$	192	0.9
36.	2.168	P. benzoquinone (Alkaloid)	$C_{14}H_{13}O_3$	228	1.1
37.	5.481	Betulin acid triterpenoids (flavonoids)	$C_{30}H_{50}O_2$	442.2	30.0
38.	5.481	Patchonile acohol (alcohol)	$C_{15}H_{26}NO$	222	4.5

al., 2024; Ibrahim & Idoko, 2023; Mankilik *et al.,* 2021; Rashad *et al.,* 2024), confirming these compounds as characteristic of the plant.

Prediction of Biological Activities of *A. aspera* Shoot Phytochemicals

Table 2 presents the LC-MS analysis of *A. aspera* shoot phytochemicals, detailing retention time (RT/min), molecular formula, molecular weight, and peak area (%), indicating compound concentration. Pentacontanol phosphate esters, oleanolic acid, and betaine exhibited 100% peak areas, followed by gypsogenic acid (99%) and chikusetsusaponin IVa (87%). Other notable compounds and their peak areas included rotundioside B (37.03%), 5,7-dimethoxyflavone-4-O-α-6-rhamnopyranosyl glycoside (33.4%), betulinic acid (30%), α-spinasterol glycoside (29.5%), dexapanthenol (16.26%), eugenol (16.2%), and acetoxy-6-benzoyloxy apangamide (16.7%). A chemical similarity search on PubChem identified eighteen of these compounds, providing their PubChem CID, molecular formula, molecular weight, and canonical SMILES. Table 2 also presents predicted antimalarial activities, including direct antiplasmodial action and plasmepsin inhibitory activities. Of the eleven compounds assessed, 4-(3-hydroxy-1-propenyl-2-methoxyphenol) and chikusetsusaponin IVa were predicted to exhibit antiplasmodial activity, while 4-(3-hydroxy-1-propenyl-2-methoxyphenol) and dexapanthenol were predicted to inhibit plasmepsin II. Rotundioside B showed no predicted antiplasmodial or enzyme inhibitory activity.

Table 2: Chemical Similarity Search of *Achyranthesaspera* Shoot Phytochemicals fromPubChem Data Based

S/N	Compounds	PubChem CID	Molecular Formula	Molecular weight (g/mol)	Canonical SMILES
1	4-(3-hydroxy-1-propenyl-2-methoxy (phenol)	9983	$C_{20}H_{40}O$	180	COC1=C(C=CC(=C1)C=CCO)O
2	Alpha-ionone (volatile oil)	5282108	$C_{13}H_{20}$	192	CC1=CCCC(C1C=CC(=O)C)(C)C
3	Alpha-spinasterol-3-glycoside	12960505	$C_{35}H_{58}O_6$	574	CCC(C=CC(C)C1CCC2C1(CCC3C2=CCC4C3(CCC(C4)OC5C(C(C(C(O5)CO)O)O)O)C)C)C(C)C

4	Betaine (flavonoid)	247	$C_5H_{11}NO_2$	550	C[N+](C)(C)CC(=O)[O-]
5	Betulin (flavonoid)	72326	$C_{30}H_{50}O_2$	442.2	CC(=C)C1CCC2(C1C3CCC4C5(CCC(C(C5CCC4(C3(CC2)C)C)(C)C)O)C)CO
6	Cauasapogenin	73299	$C_{30}H_{48}O_4$	472	CC1(CCC2(CCC3(C(=CCC4C3(CCC5C4(CCC(C5(C)CO)O)C)C)C2C1)C)C(=O)O)C
7	Chikutsesusaponiniva	13909684	$C_{42}H_{66}NO_4$	794	CC1(CCC2(CCC3(C(=CCC4C3(CCC5C4(CCC(C5(C)C)OC6C(C(C(C(O6)C(=O)O)O)O)O)C)C)C2C1)C)C(=O)OC7C(C(C(C(O7)CO)O)O)O)C
8	Dexapanthenol	131204	$C_9H_{19}NO_4$	205	CC(C)(CO)C(C(=O)NCCCO)O
9	Eugenol acetate (phenol)	7136	$C_{12}H_{14}O_3$	206	CC(=O)OC1=C(C=C(C=C1)CC=C)OC
10	Gypsogenic acid	15560324	$C_{30}H_{46}O_5$	486	CC1(CCC2(CCC3(C(=CCC4C3(CCC5C4(CCC(C5(C)C(=O)O)O)C)C)C2C1)C)C(=O)O)C
11	Gypsogenin-3-0-D glucoronide (saponin)	3086515	$C_{36}H_{54}O_{10}$	646	CC1(CCC2(CCC3(C(=CCC4C3(CCC5C4(CCC(C5(C)C=O)OC6C(C(C(C(O6)C(=O)O)O)O)O)C)C)C2C1)C)C(=O)O)C
12	Lupeol (triterpene)	259846	$C_{30}H_{50}O$	426	CC(=C)C1CCC2(C1C3CCC4C5(CCC(C(C5CCC4(C3(CC2)C)C)(C)C)O)C)C
13	Lutein	5281243	$C_{40}H_{56}O_2$	568	CC1=C(C(CC(C1)O)(C)C)C=CC(=CC=CC(=CC=CC=C(C)C=CC=C(C)C=CC2C(=CC(CC2(C)C)O)C)C)C
14	Oleonolic acid (triterpeneaglyconesaponin)	10494	$C_{30}H_{48}O_3$	456	CC1(CCC2(CCC3(C(=CCC4C3(CCC5C4(CCC(C5(C)C)O)C)C)C2C1)C)C(=O)O)C
15	P-benzoquinone (Alkaloid)	4650	$C_{14}H_{13}O_3$	228	C1=CC(=O)C=CC1=O
16	Phytol (deterpene alcohol)	5280435	$C_{20}H_{40}O$	296	CC(C)CCCC(C)CCCC(C)CCCC(=CCO)C
17	Rotundioside B	441943	$C_{54}H_{87}O_{26}S$	1184.3	CC1(CCC2(CCC3(C(=CCC4C3(CCC5C4(CCC(C5(C)C)OS(=O)(=O)[O])C)C)C2C1)C)C(=O)C6C(C(C(C(O6)COC7C(C(C(C(O7)CO)O)O)OC8C(C(C(C(O8)COC9C(C(C(C(O9)CO)O))O)O)O)O)O)O)O)C
18	Spathulenol	92231	$C_{15}H_{29}O$	220	CC1(C2C1C3C(CCC3(C)O)C(=C)CC2)C

In Silico Molecular Docking Study

The molecular docking results and interactions with residual amino acids are presented in Table 3, Table 4, and Figure 10. The antimalarial potential of each compound was assessed based on binding energy and amino acid interactions. Binding energy served as a measure of conformational stability between the receptors (Aspartic proteases) and ligands (compounds from *A. aspera* shoot). A lower negative binding energy indicated a stronger interaction between the ligand and the protein (Trott & Olson, 2010).

Table 3 presents the binding energies and enzyme pocket residue interactions following docking. The results predicted that the phytochemicals could inhibit one or more target proteins, with Rotundioside B and 4-(3-hydroxy-1-propenyl-2-methoxy) demonstrating the strongest interactions. These compounds interacted with all three proteins (Plasmepsin I, II, and IV), with binding energies of -5.3, -6.7, and -4.9 kcal/mol, and -4.4, -6.9, and -5.4 kcal/mol, respectively.

For comparison, chloroquine and artemisinin exhibited binding energies of -5.2, -7.5, -5.7 kcal/mol and -5.9, -6.4, -6.0 kcal/mol, respectively. Rotundioside B showed stronger binding to Plasmepsin I than chloroquine, while both Rotundioside B and 4-(3-hydroxy-1-propenyl-2-methoxy) exhibited stronger binding to Plasmepsin II than artemisinin. Additionally, 4-(3-hydroxy-1-propenyl-2-methoxy) (phenol) bound more effectively to Plasmepsin II than chloroquine and demonstrated a binding capacity comparable to artemisinin (Trott & Olson, 2010; Ashwini *et al.,* 2017).

Table 3: In Silico Prediction of Antiprotozoal (*Plasmodium*) and Plasmepsins Inhibitory Activities of *Achyranthes aspera* Shoot

Phytochemicals and Standard Drugs (Chloroquine and Artemisinin) by Predicted Activity Spectra of Substances (PASS)				
S/N	**Compound Name**	**Pa**	**Pi**	**Biological Activity**
1.	4-(3-hydroxy-1-propenyl-2-methoxy (phenol)	0.241	0.029	Antiprotozoal (*Plasmodium*)
		0.075	0.015	Plasmepsin II inhibition
2.	Chikutsesusaponiniva	0.227	0.037	Antiprotozoal (*Plasmodium*)
		-	-	-
3	Dexapanthenol	-	-	-
		0.076	0.015	Plasmepsin II inhibition
4.	Rotundioside B	NR	NR	NR
		NR	NR	NR
5.	Chloroquine (Standard drug)	0.898	0.002	Antiprotozoal (*Plasmodium*)
		0.055	0.054	Plasmepsin II inhibition
6.	Artemisinin (Standard drug)	0.954	0.001	Antiprotozoal (*Plasmodium*)
		-	-	-

Pa = Probability "to be active" and Pi = probability "to be inactive" - = absent, NR = not responding due to negative charge

Table 4: Predicted Interaction of Aspartic Protease (Plasmepsins) with*Achyranthesaspera* Shoot Phytochemicals and their Amino Acid Residues

S/N	**Compounds**	**Plasmepsin 1**		**Plasmepsin 1I**		**Plasmepsin 1V**	
		Binding Energies (kcal/mol)	**Ligand-Amino acid interactions**	**Binding Energies (kcal/mol)**	**Ligand-Amino acid interactions**	**Binding Energies (kcal/mol)**	**Ligand-Amino acid interactions**
1.	Rotundioside B	-5.3	Asn37B, Ser129B, Tyr69B, Lys70B	-6.7	Tyr192A, Gyl216A, Ile14A	-4.9	Thr54A, Thr104B, Lys107B, Ala283B, His56A, Lys92A, Ser 103B, Thr 104B, Gly117A, Asp121A, Asp279B
2.	4-(3-hydroxy-1-propenyl-2-methoxy (phenol)	-4.4	Gly131B, Val71B, Phe48B, Ile130B	-6.9	Met75A, Trp41A, Phe111A	-5.4	Lys101B, Glu1119A, Phe16A, Ile86A
3.	Dexapanthenol	-4.4	Met73B, Val71B, Asn37B, Ala36B, Ser132B	-4.2	Asp214A, Thr217A, Gly36A, Asp34A	-4.5	Phe16A, Leu98B, Ser118A, Asp87A, Gly117A

4.	Chloroquine drug	-5.2	Val71B, Met73B, Phe84B, Asn37B, Glu72B	-7.5	Trp41A, Pro43A, Tyr77A, Val82A, Val105A, Thr108A, Phe111A, Ile123A, Asp34A, Ser37A	-5.7	Phe16A, Glu119A, Leu98B, Lys161B, Asp87A, Gly117A
5.	Artemisinin drug	-5.9	Lys86B, Val133B, Lys100B	-6.4	Ser218A	-6.0	Lys107B, Lys111B, Leu 284B

KEY: Gln- Glutamine, Tyr- Tyrosine, Lys- Lysine, Ser – Serine, Gly- Glycine, Val –Valine, Phe – Phenylanine, Ile – Isoleucine, Met – Methionine, Ala – Alanine, Thr – Threonine, Trp – Tryptophan, Pro – Proline, His – Histidine, Leu – Leucine, Glu – Glutamic acid, Cys – Cystiene

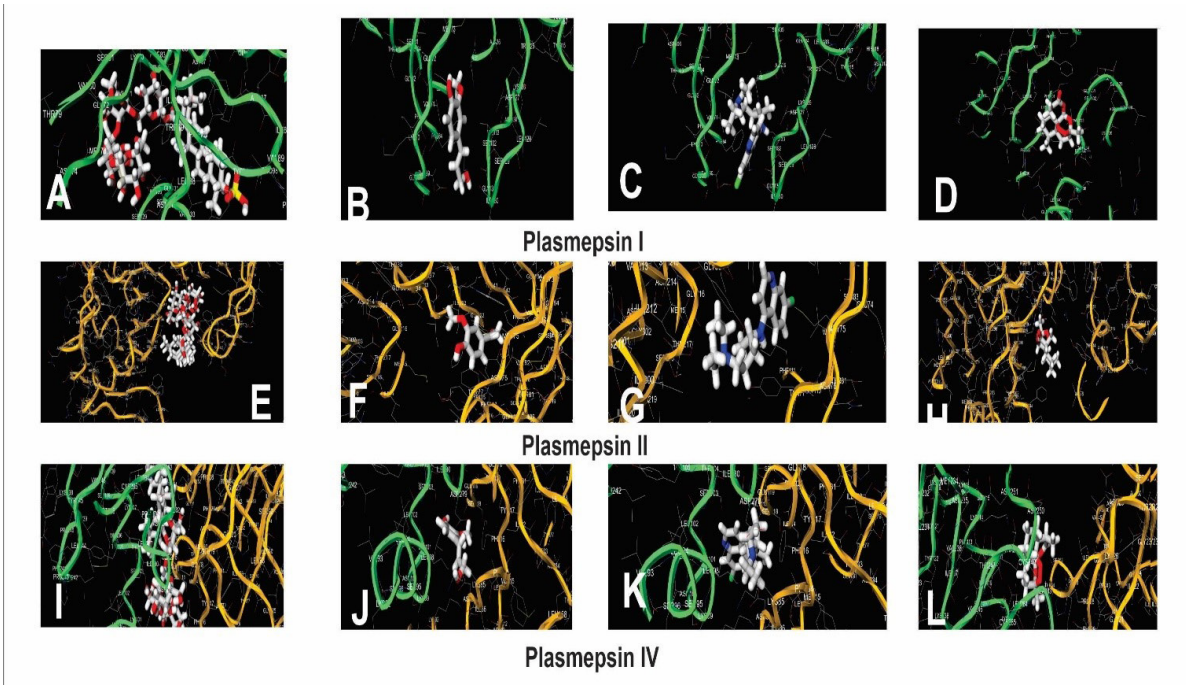

Figure 10: Molecular Interactions of Rotundioside B (A, E and I), 4-(3-hydroxy-1-propenyl-2-methoxy (phenol) (B, F and J), Chloroquine (C, G and K) and Artemisinin (D, H and L) with Plasmepsin I, II and IV respectively.

In Silico Pre-Clinical Testing

The ADMET predictions revealed that all analyzed compounds exhibited favorable drug-like properties, as evidenced by their oral bioavailability, appropriate hydrogen bond interactions, and suitable lipophilicity and TPSA values (Table 5). Specifically, rotundioside B

Table 5: Prediction of Adsorption, Distribution, Metabolism, Excretion and Toxicity of *Achyranthesaspera* Shoot Phytochemicals

S/N	Compound Name	Heavy Atom	Hetero Atom	Solubility (mg/L)	Oral (Bioavailability (EGAN)	Oral (Bioavailability (VEBER)	Ratio (H/C)	3-75	Status
1.	4-(3-hydroxy-1-propenyl-2-methoxy (phenol)	13	06	22863.0	Good	Good	0.30	Warming	Accepted
2	Chikutsesusaponiniva	56	14	695.8	Good	Good	0.33	Warming	Accepted

3	Dexapanthenol	14	05	176739.5	Good	Good	0.56	Good	Accepted
4.	Rotundioside B	81	27	3491.9	Low	Low	0.50	Good	Accepted

FAF represents the Free ADMET Adaptable Tool, EGAN represents Egan's Rule (Topological Polar Surface Area (TPSA) > 104 Å² or number of rotatable bonds > 10), VEBER represents Veber's Rule (Topological Polar Surface Area (TPSA) > 131.6 Å² or LogP > 5), and H/C represents the Hydrogen-to-Carbon Atom Ratio.

Table 6: Prediction of Drug Likeness Properties of *Achyranthes aspera* Shoot Phytochemicals

S/N	Compounds						
		Molecular Mass less than 500 Dalton	**Hydrogen Bond Donor Less than 5**	**Hydrogen Bond Acceptor less than 10**	**LOGP High lipophilicity expressed as Log P less than 5**	**Molar Refractivity less should be between 40-130**	**Status**
1	4-(3-hydroxy-1-propenyl-2-methoxy (phenol)	180	2	3	1.38	46.45	Accepted
2	Chikutsesusaponiniva	205	4	4	1.51	55.40	Accepted
3	Dexapanthenol	205	0	3	2.40	54.10	Accepted
4	Rotundioside B	312	5	6	-0.05	77.15	Accepted

Molecular weight acceptable range: <500, Hydrogen bond acceptor (HBA) range: ≤10
Hydrogen bond donor (Hbd) ranges acceptable range: ≤5, Lipophilicity (LogPo/w acceptable range: <5
Molar refractivity should be between 40 to 130
Rule of Five (ROF): Number of Violation of Lipinskis rule of five; recommended range: 0

and 4-(3-hydroxy-1-propenyl-2-methoxyphenol) fulfilled the criteria for drug-likeness, indicating their potential as promising lead compounds (Table 6). These findings are in accordance with the Lipinski rule of five, which predicts oral activity based on relevant molecular properties (Lipinski *et al.*, 2001).

CONCLUSION

The fractionated extracts of *Achyranthes aspera* demonstrate significant antimalarial potential with the chloroform fraction particularly effective in reducing *Plasmodium berghei* parasitemia in vivo. The identification of bioactive compounds with inhibitory activity against Plasmepsins I, II, and IV through molecular docking strengthens the therapeutic significance of this medicinal plant. Additionally, in silico ADMET analysis has confirmed the drug-like properties and favorable pharmacokinetic characteristics of key phytochemicals. These results underscore *A. aspera* as a valuable source of novel antimalarial compounds, necessitating further studies to explore its clinical efficacy and mechanisms of action for future pharmaceutical applications.

Funding

This research was financially supported by the University of Jos through the African Center of Excellence in Phytomedicine Research and Development, in collaboration with the World Bank (ACEPRD/UJ/028).

Ethical Statement

This study received ethical approval from the Department of Pharmacognosy Ethics Committee, Faculty of Pharmaceutical Sciences, University of Jos (Ethical Number: UJ/FPS/F17-00379). The experimental protocol complied with national and international laws and guidelines for using laboratory animals. All the authors affirm that the research is original, free from plagiarism, and that all findings are accurately reported without fabrication or falsification of data.

REFERENCES

Alam, M. T., Karim, M. M., & Khan, S. N. (2004). Antibacterial activity of different organic extracts of *Achyranthes aspera* and Cassia alata. *Journal of Scientific Research, 1*, 393–398.

Ashley, E. A., & *et al.* (2014). Spread of artemisinin resistance in *Plasmodium falciparum*. *New England Journal of Medicine, 371*(5), 411–423.

Ashwini, S., Varkey, S. P., & Shantaram, M. (2017). In silico docking of polyphenolic compounds against caspase-3-Hela cell line protein. *International Journal of Drug Development & Research, 9*, 28–32.

Balunas, M., & Kinghorn, A. (2005). Drug discovery from medicinal plants. *Life Sciences, 78*(5), 431–441.

Berry, C. (1997). New targets for antimalarial: The plasmoepsin, malaria parasite aspartic proteases. *Biochemical Education, 25*(4), 191–194.

Burkill, H. M. (1985). Lasiurus hirsutus (Forssk) Boiss (family Poaceae) In *The useful plants of West Tropical Africa* (2nd ed.). Royal Botanic Gardens.

CDC - DPDx - Diagnostic Procedures - Blood Specimens. (2019, January 8). Cdc.gov. https://www.cdc.gov/dpdx/diagnosticprocedures/blood/microexam.html?utm_source=chatgpt.com

Chileh-Chelh, T., López-Ruiz, R., García-Cervantes, A. M., Rodríguez-García, I., Rincón-Cervera, M. A., Ezzaitouni, M., & Guil-Guerrero, J. L. (2024). Cytotoxicity and chemotaxonomic significance of saponins from wild and cultured asparagus shoots. *Molecules, 29*(14), 3367. https://doi.org/10.3390/molecules29143367

Chilombe, M. B., McDermott, M. P., Seydel, K. B., Mathews, M., Mwenechanya, M., & Birbeck, G. L. (2022). Aggressive antipyretics in central nervous system malaria: Study protocol of a randomized-controlled trial assessing antipyretic efficacy and parasite clearance effects (Malaria FEVER study). *PLoS ONE, 17*(10), e0268414. https://doi.org/10.1371/journal.pone.0268414

Clarke, A. (2004). Is there a universal temperature dependence of metabolism? *Functional Ecology, 18*(2), 252–256. https://doi.org/10.1111/j.0269-8463.2004.00842.x

Coombs, G. H., Goldberg, D. E., Klemba, M., & *et al.* (2001). Aspartic properties of *Plasmodium falciparum* and other parasitic protozoa as drug targets. *Trends in Parasitology, 17*(11), 523–527.

Davkova, I., Zhivikj, Z., Kukić-Marković, J., Cvetkovik-Karanfilova, I., Stefkov, G., Kulevanova, S., & Karapandzova, M. (2024). Natural products in the management of obesity. *Arhiv za Farmaciju, 74*(3), 298–315. https://doi.org/10.5937/arhfarm74-50438

Dondorp, A. M., & *et al.* (2009). Artemisinin resistance in *Plasmodium falciparum* malaria. *New England Journal of Medicine, 361*(5), 455–467.

Elumalai, E. K., Chandrasekaran, N., Thirumalai, N., Sivakumar, C., Theresa, S. V., & David, E. (2009). *Achyranthes aspera* leaf extract inhibited fungal growth. *International Journal of Pharmaceutical Research, 1*(4), 1576–1579.

Fidock, D. A., Eastman, R. T., Ward, S. A., & *et al.* (2008). Recent highlights in antimalarial drug resistance and cleaner apply research. *Trends in Parasitology, 24*(2), 537–544.

Francis, S. E., Sullivan, D. J., & Goldberg, and D. E. (1997). Hemoglobin Metabolism in The Malaria Parasite*plasmodium Falciparum. Annual Review of Microbiology, 51*(1), 97–123. https://doi.org/10.1146/annurev.micro.51.1.97

Ibrahim, M., & Idoko, A. S. (2023). Phytochemical analysis of hexane, chloroform, ethyl acetate, ethanol, and aqueous extracts of Azanza garckeana leaf. *Sahel Journal of Life Sciences FUDMA, 1*(1), 25–31. https://doi.org/10.33003/sajols-2023-0101-003

Jain, J. B., Kumane, S. C., & Bhattacharya, S. (2006). Medicinal flora of Madhya Pradesh and Chhattisgarh: A review. *Indian Journal of Traditional Medicine, 5*(2), 237–242.

Kamau, E., S. Campino, L. Amenga-Etego, Drury, E., D. Ishengoma, Johnson, K., D. Mumba, M. Kekre, W. Yavo, Mead, D., M. Bouyou-Akotet, T. Apinjoh, L. Golassa, M. Randrianarivelojosia, B. Andagalu, O. Maiga-Ascofare, A. Amambua-Ngwa, P. Tindana, A. Ghansah, & MacInnis, B. (2014). K13-Propeller Polymorphisms in *Plasmodium falciparum* Parasites From Sub-Saharan Africa. *The Journal of Infectious Diseases*. https://doi.org/10.1093/infdis/jiu608

Khodade, P., Prabhu, R., Chandra, N., Raha, S., & Govindarajan, R. (2007). Parallel implementation ofAutoDock. *Journal of Applied Crystallography, 40*(3), 598–599. https://doi.org/10.1107/s0021889807011053

Kumar, S. V., Sankar, P., & Varatharajan, R. (2009). Anti-inflammatory activity of roots of *Achyranthes aspera*. *Pharmaceutical Biology, 47*(10), 973–975.

Lagorce, D., Bouslama, L., Becot, J., Miteva, M. A., & Villoutreix, B. O. (2017). FAF-Drugs4: Free ADME-tox filtering computations for chemical biology and early stages drug discovery. *Bioinformatics, 33*(22), 3658–3660. https://doi.org/10.1093/bioinformatics/btx491

Lipinski, C. A., Lombardo, F., Dominy, B. W., & Feeney, P. J. (2001). Experimental and computational approaches to estimate solubility and permeability in drug discovery and development settings. *Advanced Drug Delivery Reviews, 46*(1–3), 3–26. https://doi.org/10.1016/S0169-409X(00)00129-0

Liu, S., Gluzman, I., Drew, M., & Goldberg, D. (2004). The role of *Plasmodium falciparum* food vacuole plasmepsin. *Journal of Biological Chemistry, 280*(2), 1432–1437.

Longdet, I. Y., Mary, M. M., Maria, O. O., & David, I. E. (2019). Copyright© 2019 by Academic Publishing House Researcher sro Published in the Slovak Republic Russian Journal of Biological Research. *Russian Journal of Biological Research, 6*(1).

López-Yerena, A., Perez, M., Vallverdú-Queralt, A., & Escribano-Ferrer, E. (2020). Insights into the binding of dietary phenolic compounds to human serum albumin and food-drug interactions. *Pharmaceutics, 12*(11), 1123. https://doi.org/10.3390/pharmaceutics12111123

Mankilik, M. M., Longdet, I. Y., & Luka, C. D. (2021). Evaluation of *Achyranthes aspera* shoot extract as an alternative therapy for malaria. *The Journal of Basic and Applied Zoology, 82*(1). https://doi.org/10.1186/s41936-021-00211-4

Menard, C., Hodes, G. E., & Russo, S. J. (2016). Pathogenesis of depression: Insights from human and rodent studies. *Neuroscience, 321*, 138–162.

Moura, P., Dame, J., & Fidock, D. (2009). Role of *Plasmodium falciparum* digestive vacuole plasmepsin in the specificity and antimalarial mode of action of cysteine and aspartic protease inhibitors. *Antimicrobial Agents and Chemotherapy, 53*(12), 4968–4978.

National Research Council. (2011). *Guide for the care and use of laboratory animals* (8th ed.). National Academies Press. https://grants.nih.gov/grants/olaw/guide-for-the-care-and-use-of-laboratory-animals.pdf

Noedl, H., Se, Y., Schaecher, K., Smith, B. L., Socheat, D., & Fukuda, M. M. (2008). Evidence of artemisinin-

resistant malaria in western Cambodia. *New England Journal of Medicine, 359*(24), 2619-2620.

Pandey, K. C., & Dixit, R. (2012). Structure function of *Plasmodium falciparum*: Malarial cysteine proteases. *Journal of Tropical Medicine,* 1–11.

Priya, C. I., Kumar, G., Karthik, L., & Rao, K. V. (2010). Antioxidant activity of *Achyranthes aspera* Linn. stem extracts. *Pharmacology Online, 2*, 228–237.

Protsiv, M., Ley, C., Lankester, J., Hastie, T., & Parsonnet, J. (2020). Decreasing human body temperature in the United States since the Industrial Revolution. *eLife, 9*. https://doi.org/10.7554/elife.49555

Rao, Y. V., Govinda, R. D., Babu, G. S., & Rao, R. A. (2002). Immunomodulatory activity of *Achyranthes aspera* on the elicitation of antigen-specific murine antibody response. *Pharmaceutical Biology, 40*(3), 175–178.

Rashad, M., Adil, M. A., Siddique, M. B., Peerzadah, S., & Saadullah, M. (2024). Antioxidant and pharmacognostic evaluation of *Achyranthes aspera*: Therapeutic potential and analytical validation of secondary metabolites. *Australian Herbal Insight, 7*(1), 1–14. https://doi.org/10.25163/ahi.719692

Rasmussen, C., Alonso, P., & Ringwald, P. (2021). Current and emerging strategies to combat antimalarial resistance. *Expert Review of Anti-Infective Therapy, 20*(3), 1–20. https://doi.org/10.1080/14787210.2021.1962291

Rosenthal, P. (1998). Proteases of malaria parasites: New targets for chemotherapy. *Emerging Infectious Diseases, 4*(1), 49–57.

Ryley, J. F., & Peters, W. (1970). The antimalarial activity of some quinolone esters. *Annals of Tropical Medicine & Parasitology, 64*(2), 209-222.

Saglam, K., & Sekerler, T. (2024). A comprehensive review of the anti-obesity properties of medicinal plants. *Pharmedicine Journal, 1*(2), 46–67. https://doi.org/10.62482/pmj.10

Sahib, N. G., Saari, N., Ismail, A., Khatib, A., Mahomoodally, F., & Hamid, A. A. (2012). Plants' metabolites as potential antiobesity agents. *The Scientific World Journal, 2012,* 1–8. https://doi.org/10.1100/2012/436039

Saurabh, S., Singh, P., Mishra, G., Jha, K. K., & Khosa, R. L. (2011). *Achyranthes aspera* – An important medicinal plant: A review. *Journal of Natural Product and Plant Resources, 1*(1), 1–14.

Shibeshi, M. A., Kifle, Z. D., & Atnafie, S. A. (2020). Antimalarial drug resistance and novel targets for antimalarial drug discovery. *Infection and drug resistance,* 4047-4060.

Tiwari, P., Kaur, M. and Kaur, H. (2011) Phytochemical Screening and Extraction: A Review. *Internationale Pharmaceutica Sciencia, 1*, 98-106.

Tiwari, P., Nayak, P., Prusty, S. K., & Sahu, P. K. (2018). Phytochemistry and pharmacology of Tinospora cordifolia: A review. *Sys Rev Pharm, 9*(1), 70–78.

Trott, O., & Olson, A. J. (2010). AutoDock Vina: Improving the speed and accuracy of docking with a new scoring function, efficient optimization, and multi-threading. *Journal of Computational Chemistry, 31*, 455–461.

WHO. (2021). *World malaria report 2021*. Retrieved March 2, 2025, from Who.int website: https://www.who.int/teams/global-malaria-programme/reports/world-malaria-report-2021

Wilson, D. W., Langer, C., Goodman, C. D., McFadden, G. I., & Beeson, J. G. (2013). Defining the Timing of Action of Antimalarial Drugs against *Plasmodium falciparum*. *Antimicrobial Agents and Chemotherapy, 57*(3), 1455–1467. https://doi.org/10.1128/aac.01881-12

Yared, D., Mekonnen, Y., & Debella, A. (2012). In vivo antimalarial activities of fractionated extracts of Asparagus africanus in mice infected with *Plasmodium berghei*. *Pharmacologyonline, 3*, 88-94.